Tellus (1985), 37A, 233–248

Sensitivity of an energy balance climate model with predicted snowfall rates

By KENNETH P. BOWMAN*, *Geophysical Fluid Dynamics Program, Princeton University, P.O. Box 308, Princeton, New Jersey 08540, USA*

(Manuscript received June 15; in final form December 10, 1984)

ABSTRACT

A two-level zonally-averaged seasonal energy balance model with separate land and ocean temperatures and an explicit surface energy budget is used to study the effects of the snowfall rate on the extent of snow cover and ice sheets. Sensitivity experiments are performed both with and without ice sheets and with two different snowfall parameterizations. When snowfall rates are prescribed independent of latitude, higher snowfall rates increase the area of snow cover but reduce the sensitivity of the snow line to changes of the solar constant. To eliminate arbitrary assumptions about the snowfall rate, a relationship between the atmospheric transports of water vapour and sensible heat is derived and tested against observations. The relationship obtained is used to predict the meriodional transport of water vapour in the model, from which the precipitation and snowfall are calculated. The response of the hydrologic cycle to changes of the solar constant is qualitatively similar to that found in general circulation models. The snow line is more sensitive with the predicted precipitation than with the prescribed precipitation because the predicted precipitation rate increases toward the equator. When ice sheets are included, they are larger than permanent snow cover under the same conditions because the cold surface temperatures at high elevations on the ice sheet inhibit melting. Feedback effects of the ice sheets are small, in part because they are limited to 30% of a latitude circle in this model.

1. Introduction

Studies of deep-sea sediment cores have shown that the quasiperiodic changes of the Earth's orbital parameters and the resulting redistribution of insolation have affected the global ice volume during the last several hundred thousand years (Milankovitch, 1941; Hays et al., 1976). Still, much of the variance of the ice volume, notably the dominant periodicity of ~100 thousand years, remains unexplained. The purpose of this paper, however, is not to explore the origin of the 100 thousand year cycle or to ask whether the orbital variations influence the climate, but to investigate how changes in insolation (or perhaps in atmospheric CO_2) produce changes in the climate, especially in the extent of snow and ice.

The sensitivity of snow and ice cover to changes of other climatic parameters is of fundamental importance in climate problems. Numerous models have been used to study the sensitivity of snow and ice cover or to simulate the ice ages, ranging from extremely simple zero- and one-dimensional energy balance models (EBMs) (see North et al., 1981 for a review); to more complex EBMs with seasonally varying insolation, detailed physical parameterizations (Suarez and Held, 1979), and realistic geography (North et al., 1983); to full three-dimensional general circulation models (GCMs) (Williams et al., 1974; Wetherald and Manabe, 1975; Gates, 1976). Unfortunately, GCMs are too expensive to use for extensive sensitivity experiments, and the results may be difficult to interpret. Energy balance models are more economical and easier to understand because complex climatic processes are approximated by simpler parameterizations. However, because the accuracy of the parameterizations is largely unknown, simple models are most useful for analyzing individual processes and feedback mechanisms and as aids in understanding results from more

* Present address: Laboratory for Atmospheres, Code 613, Goddard Space Flight Center, Greenbelt, MD 20771 U.S.A.

sophisticated models. This paper will describe a method of parameterizing snow cover, ice sheets, and albedo in energy balance models, and the effects of the parameterization on the model climate.

In the simplest EBMs snow and ice cover are simulated by a temperature-dependent planetary albedo (Budyko, 1969; Sellers, 1969; Held and Suarez, 1974; North, 1975). The temperature-dependent albedo can lead to a positive feedback between the temperature and the albedo, making the model snow cover and temperature very sensitive to perturbations of the solar constant. The albedo parameterization is important in simple EBMs because it can so strongly influence the model sensitivity.

The temperature-dependent albedo is undoubtedly unrealistically simple, but it is convenient for many types of studies. In reality, of course, the areal extent of snow cover or sea ice is not controlled by temperature alone. Also, many model experiments have been conducted with snow cover only, although ice sheets can introduce new effects into the models (Bowman, 1982). And while ice sheets change only on a time scale of decades or longer, snow cover and sea ice change extensively during the seasons. A realistic model must therefore predict the seasonal cycle of snow and ice cover, as well as ice sheet size, in order to correctly determine the surface albedo.

Energy balance models have been constructed with simple snow budgets, but snowfall rates have remained external parameters. Pollard et al. (1980) used the observed precipitation rate and an empirical snowmelt formula based on observations. Suarez and Held (1979) adapted some methods from general circulation models by computing a surface energy balance from simplified radiation calculations and predicting melt rates. Snow was assumed to fall at the observed zonal-mean precipitation rate whenever the temperature was below freezing. A simple method was also used to predict sea ice thickness. Birchfield et al. (1982) used a similar model coupled to a dynamic ice sheet model, but precipitation rates were prescribed in a similar manner as external parameters.

Using the observed precipitation rates may be appropriate if the climate is perturbed only slightly, so that the precipitation distribution changes little. However, climatic changes on the scale of the ice ages, when large ice sheets extended into middle latitudes, probably involved significant changes in the zonal-mean precipitation.

This paper will described a simple parameterization for the zonal-mean snowfall rate and discuss its effects on the climate of a seasonal, two-level, diffusive energy balance model both with and without large polar ice sheets. The energy balance model is essentially that of Suarez and Held (1979) mentioned above. This model was chosen because it includes the detailed parameterizations of the surface energy balance and radiative fluxes needed to calculate the melt component of the snow budget and the evaporation and sublimation. The snowfall parameterization is derived in Section 2.2, and the method of coupling the energy balance model to a simple ice sheet model is described in section 2.3.

The sensitivity of the model without ice sheets is discussed first in Part 3. Some simple experiments with prescribed precipitation rates are performed to aid in understanding the results obtained with the model predicted snowfall.

In Part 4 the sensitivity of the model with polar ice sheets is compared to the sensitivity with snow cover alone. The explicit snowfall parameterization illuminates some important differences between the climatic effects of snow cover and ice sheets. Again, sensitivity experiments are performed with both prescribed precipitation rates and with predicted snowfall.

Some implications of the model results for the present climate and for ice age theories are discussed in Part 5.

2. Model description

2.1. *The energy balance model*

The model used in this study has been thoroughly described in Suarez and Held (1979), Suarez (1976), and Held and Suarez (1978), so only a summary is given here. The dependent variables are the potential temperatures at 250 and 750 mb, Θ_1 and Θ_2 respectively. With the meridional transport of energy simulated by diffusion, the model equations are

$$\frac{\partial \Theta_k}{\partial t} = \frac{D}{a^2 \cos\theta} \frac{\partial}{\partial \theta} \cos\theta \frac{\partial \Theta_k}{\partial \theta} + \left(\frac{p_0}{p_k}\right)^{\kappa} \frac{Q_k}{c_p m_a}. \quad (1)$$

The subscript k identifies the pressure level. θ, p, and t are latitude, pressure, and time respectively.

Q_k is the sum of all diabatic processes. Other symbols and the numerical values of parameters are given in Table 1.

The diabatic processes are divided into shortwave and longwave radiation, Q^{sw} and Q^{lw}, fluxes of sensible and latent heat from the surface, Q^{sh} and Q^{lh}, and heat exchanged between the two atmospheric layers by convective adjustment, Q^{ca}. The total heating at each level is

$$Q_1 = f(\theta)(Q_1^{sw} + Q_1^{lw})_L + (1-f(\theta))(Q_1^{sw} + Q_1^{lw})_O + Q^{ca}, \quad (2a)$$

and

$$Q_2 = f(\theta)\,(Q_2^{sw} + Q_2^{lw} + Q^{sh} + Q^{lh})_L \; (1 - f(\theta))\,(Q_2^{sw} + Q_2^{lw} + Q^{sh} + Q^{lh})_O - Q^{ca}. \quad (2b)$$

Subscripts L and O refer to quantities computed over land and ocean, and $f(\theta)$ is the land fraction at each latitude. Land is assumed to have no heat capacity, while ocean consists of an isothermal layer 40 m deep.

The atmospheric temperature is assumed to be constant above 200 mb and to vary linearly with the logarithm of pressure between 200 mb and the surface, passing through the two predicted temperatures $T_1 = (1/4)^\kappa\, \Theta_1$ and $T_2 = (3/4)^\kappa\, \Theta_2$. Shortwave and longwave radiation fluxes were computed for different values of Θ_1, Θ_2, surface temperature T_*, and mean solar zenith angle $\bar{\zeta}$ by using an 18-level radiative transfer model (Manabe and Strickler, 1964; Stone and Manabe, 1968). The relative humidity profile and cloud amounts are given in Manabe and Wetherald (1967). Shortwave fluxes are tabulated as functions of mean atmospheric temperature $\bar{\Theta} = (\Theta_1 + \Theta_2)/2$, lapse rate $\hat{\Theta} = (\Theta_1 - \Theta_2)/2$, and $\bar{\zeta}$. Longwave fluxes at the surface, 500 mb, and the top of the atmosphere are tabulated as functions of $\bar{\Theta}$, $\hat{\Theta}$, and $\Delta T = T_* - T_s$. The surface air temperature T_s is extrapolated linearly in the logarithm of pressure from T_1 and T_2. Radiative fluxes in the model are interpolated from the tabulated values. The downward longwave flux at the surface $L\downarrow$ does not depend on T_s, so $L\downarrow$ and the downward shortwave radiation at the surface $S\downarrow$ can be computed from $\bar{\Theta}$, $\hat{\Theta}$, and $\bar{\zeta}$.

The sensible and latent heat fluxes from the surface are

$$Q^{sh} = c_d \rho c_p (T_* - T_s), \quad (3)$$

$$Q^{lh} = c_d \rho L_c (r(T_*) - \mathrm{RH}\; r(T_s)). \quad (4)$$

The relative humidity RH is 0.8, and r is the mixing ratio. When the surface is snow or ice covered, the L_c is replaced by the latent heat of sublimation $L_s = L_c + L_f$ (see Table 1). Because land has no heat capacity, T_{*L} is found by satisfying the energy balance equation at the surface

$$(1 - \alpha)S\downarrow + L\downarrow - \sigma T_{*L}^4 - Q_L^{sh} - Q_L^{lh} = 0. \quad (5)$$

The surface albedo α depends on the presence or absence of snow cover. The albedo of snow-free land and ice-free ocean is given by

$$\alpha(\theta) = \alpha_0 + \alpha_2 P_2(\theta).$$

P_2 is the second Legendre polynomial and α_0 and α_2 are equal to 0.1. The albedo therefore increases parabolically from 0.05 at the equator to 0.20 at the pole. The albedo of a snow or ice covered surface is 0.70 with no dependence on latitude, snow depth, or ice thickness.

Table 1. *Symbols and constants used in the energy balance model*

Symbol	Quantity	Value
a	radius of the Earth	$6.37 \cdot 10^6$ m
c_d	drag coefficient	$1.0 \cdot 10^{-3}$
c_p	specific heat of dry air	1004 J K^{-1} kg^{-1}
c_w	specific heat of liquid water	4218 J K^{-1} kg^{-1}
D	atmospheric diffusion coefficient	$2.25 \cdot 10^6$ m^2 s^{-1}
I_{min}	minimum sea ice thickness	1.7 cm
k_i	thermal conductivity of ice	2.2 W m^{-1} K^{-1}
L_c	latent heat of condensation of water vapor	$2.25 \cdot 10^6$ J kg^{-1}
L_f	latent heat of fusion of water	$3.34 \cdot 10^5$ J kg^{-1}
m_O	mass of the ocean mixed layer	$40 \cdot 10^3$ kg m^{-2}
m_a	mass of each layer of the atmosphere	5102 kg m^{-2}
p_0	sea level pressure	10^5 Pa
R	gas constant of dry air	287 J K^{-1} kg^{-1}
κ	R/c_p	0.286
ρ	density of air at sea level	1.28 kg m^{-3}
ρ_w	density of liquid water	10^3 kg m^{-3}
σ	Stefan-Boltzmann constant	$5.6696 \cdot 10^{-8}$ W m^{-2} K^{-4}

If (5) predicts a surface temperature greater than 0°C in the presence of snow cover, T_{*L} is set equal to 0°C and the surface energy balance is recomputed. The resulting energy flux into the surface is used to melt snow or ice.

The rate of change of the temperature of the ocean mixed layer is

$$m_O c_w \frac{dT_{*O}}{dt} = (1-\alpha)S\downarrow + L\downarrow - \sigma T_{*O}^4 - Q_O^{sh} - Q_O^{lh}. \tag{6}$$

in the absence of sea ice. When the temperature falls to 0°C, sea ice thickness I increases at the rate

$$\rho_w L_f \frac{dI}{dT} = Q^c - Q_O^m - \frac{L_f}{L_c + L_f} Q_O^s. \tag{7}$$

The surface temperature in the presence of sea ice is calculated from

$$(1-\alpha)S\downarrow + L\downarrow - \sigma T_{*O}^4 - Q_O^{sh} - Q_O^s + Q^c = 0. \tag{8}$$

Q^s is the heat flux due to sublimation. The heat flux conducted through the ice is

$$Q_c = \frac{k_I(273.16K - T_{*O})}{I + I_{min}}. \tag{9}$$

I_{min} is a minimum ice thickness used to prevent Q^c from becoming too large. If T_{*O} is greater than 273.16 K in the presence of sea ice, T_{*O} is set equal to 273.16 K, Q^c vanishes, and melting is computed as for snow cover. No snow is assumed to fall on sea ice.

Once T_* is known, the longwave fluxes at 500 mb and the top of the atmosphere are computed. The shortwave and longwave heating rates are equal to the net fluxes into each atmospheric layer. The convective adjustment scheme is described in Suarez and Held (1979).

Eq. (1) is integrated numerically with a seasonally varying insolation forcing by using the Crank-Nicholson method. The insolation is calculated for a circular orbit and an obliquity of 23.5°. The latitude and time resolution are 2° and 128 time steps per year respectively. The land fraction is set to 0.3 everywhere. Except where noted, in the following calculations the parameters are as specified in Table 1. Because the land-sea distribution and insolation are symmetric about the equator, the resulting climate is also symmetric.

Suarez and Held (1979) have discussed the sensitivity of this model with a temperature-dependent albedo and with the precipitation rate set to the observed annual-mean zonal-mean value at each latitude. To make the model somewhat less sensitive, the diffusivity and snow-free albedo are different from the values used by Suarez and Held. The model temperatures are not significantly altered as a result.

2.2. *Predicting water vapor transport and precipitation*

Assuming that the rate of change of the zonal-mean atmospheric water vapor content is small compared to the net evaporation the equation for conservation of water vapor may be written

$$\frac{1}{a\cos\theta}\frac{\partial}{\partial\theta}(\cos\theta\,\vec{Q}) = \mathrm{E} - \mathrm{P}, \tag{10}$$

where $\vec{Q}$ is the vertically-integrated meridional water vapour flux, E is the evaporation rate, and P is the precipitation rate. If $\vec{Q}$ and E are known, P can be calculated as a residual.

Because the largest portion of the meridional water vapor flux in middle latitudes is transported by transient and standing eddies, a method for predicting those quantities could be used to predict precipitation, if the evaporation is known. It is not necessary to predict precipitation in the tropics because temperatures are not sufficiently cold for snow to fall.

A relationship between the meridional fluxes of water vapour and sensible heat can be derived by expanding the specific humidity in Taylor series about $\bar{T}$, multiplying by v', taking the mean, and retaining only the first term

$$\overline{v'q'} = \left(\frac{\mathrm{RH}}{100}\frac{\varepsilon}{p}\left.\frac{\partial e_s}{\partial T}\right|_{\bar{T}}\right)\overline{v'T'} \tag{11}$$

(Mullen, 1979). Kurihara (1973, eq 2.8) used a similar formula.

Eq. (11) was tested by correlating the observed values of the left and right hand sides. Climatological values of the zonal-mean temperature, sensible heat flux, and latent heat flux were obtained from Oort (1983). The transports are divided into contributions from transient eddies (TE), stationary eddies (SE), and the mean meridional circulation (MMC). Statistics for each of the four seasons and the mean of the four seasonal values (referred to as the annual mean) were used.

For each component of the flux at each pressure level the observed values of each side of (11) were calculated. The correlation of the two quantities between 30° and 70° N latitude was calculated, and the left-hand side (y) was fit with a function of the right-hand side (x) of the form $y = bx$. This functional form ensures that the predicted water vapor transport vanishes at the poles. If the relative humidity were truly constant and (11) held exactly, b would be equal to RH/100.

The values of b and r are shown in Table 2 for the annual-mean fluxes, broken down by component and pressure level. Correlations are presented for each component separately, for all eddies (TE + SE), and for the total transport (TE + SE + MMC), Pressure levels above 500 mb have very small amounts of water vapor, so they have been omitted from the tables. Correlations for the total flux below 500 mb are shown at the bottom of the table.

Correlations for the TE component are >0.89 everywhere. The correlation decreases slightly with increasing height. The SE contribution is well correlated only very near the surface. The MMC correlation is included to aid in understanding the correlation of the total transport, though (11) would not be expected to apply. The transports by the MMC are, in fact, well correlated ($r > 0.8$) below 600 mb. Because the transient eddies and the mean meridional circulation are generally the larger contributors to the transport and are well correlated individually, the total eddy transport and the total transport are also well correlated ($r = 0.98$ for the vertical-mean transport).

The fact that b is greater than 1 for the transient eddies at most levels seems to imply relative humidities greater than 100%. Actually, the large values of b suggest that the perturbation relative humidity RH′ is well correlated with v' or T'. This could be determined only by using the original data, not the zonal-mean quantities, to calculate $\overline{RH'v'}$, $\overline{RH'T'}$, and $\overline{RH'v'T'}$. The neglected higher-order terms may also affect the correlations.

As an example, the observed and predicted annual-mean total water vapor fluxes are shown in Fig. 1. The observed sensible heat flux and the calculated value of b were used to predict the water vapor flux. The vertical-mean temperature was used to calculate the derivative of the saturation mixing ratio, and the relative humidity was assumed to be 100%. As expected, (11) works well in middle latitudes, but errs significantly in the tropics.

The correlation between the atmospheric water vapor flux and sensible heat flux (after correcting for the temperature dependence of saturation vapor pressure) is very high in middle latitudes. On the basis of these results, the meridional heat flux in the

Table 2. *Correlation between the observed annual-mean water vapor flux and sensible heat flux for each component at each pressure level for the latitude band between 30° N and 70° N. The upper number is the coefficient b of the least-squares fit to the data with a straight line through the origin. The lower number is the correlation coefficient r. Because the data are fit with a straight line of the form $y = bx$, it is possible for b and r to be of opposite sign. Data are from Oort (1983)*

Pressure (mb)	TE	SE	MMC	TE + SE	TE + SE + MMC
500	2.04	0.20	0.47	1.64	1.54
	0.89	0.58	0.24	0.85	0.79
600	1.56	0.25	0.48	1.29	1.24
	0.93	0.18	0.69	0.86	0.81
700	1.18	0.23	0.32	0.99	0.95
	0.93	0.02	0.85	0.84	0.81
800	0.92	0.49	0.40	0.88	0.78
	0.99	−0.34	0.94	0.85	0.92
900	0.82	0.68	0.39	0.87	0.50
	0.99	−0.37	0.94	0.89	0.98
1000	1.31	0.93	0.38	1.19	0.52
	0.99	0.95	0.97	0.99	0.98
550–1000	0.93	0.43	0.52	0.85	0.70
	0.95	−0.26	0.97	0.73	0.98

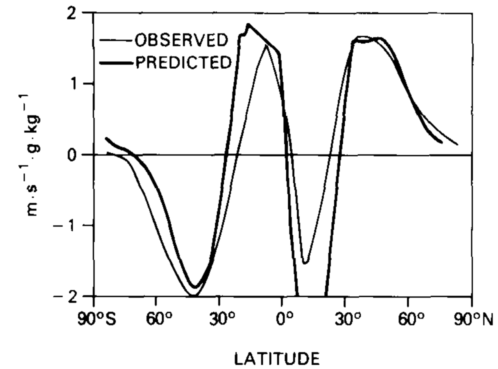

Fig. 1. Observed annual-mean vertical-mean meridional water vapor transport and the water vapor transport predicted using (11) and the observed sensible heat transport. Data are from Oort (1983).

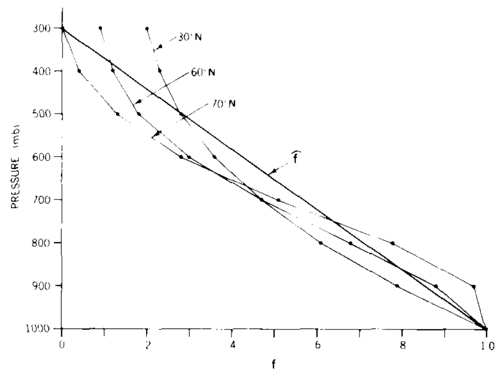

Fig. 2. Fraction of the observed total annual-mean meridional water vapor transport f above pressure level p at three different latitudes. The straight line $\hat{f}$ is the parameterization adopted for the model (eq. 12). Data are from Oort (1983).

lower layer of the model is used on the right hand side of (11) to predict the water vapor flux. The evaporation rate is known from the latent heat flux (4), and (10) is used to calculate the precipitation rate.

An additional consideration when ice sheets are included is that atmospheric water vapor is largely confined near the ground. A large ice sheet concentrates precipitation along its flanks by orographic effects. Therefore, the precipitation parameterization should be corrected to avoid overestimating the precipitation at high elevations on the ice sheet.

The vertical distribution of the water vapor flux was computed from the same statistics used to test (11). Fig. 2 shows the fraction of the water vapor transport above pressure level p, $f(p)$, for the total annual-mean transport at three different latitudes. As would be expected, at higher latitudes, the water vapor flux is entirely confined below 300 mb, while at 30 °N 20% of the transport occurs above 300 mb.

In the model these curves are approximated by a function of the form

$$\hat{f}(p) = \begin{cases} 0 & p \leqslant 300 \text{ mb}, \\ \dfrac{p - 300 \text{ mb}}{700 \text{ mb}} & 300 \text{ mb} < p < 1000 \text{ mb}, \\ 1 & p \geqslant 1000 \text{ mb}. \end{cases} \quad (12)$$

By assuming that the ice sheet entirely blocks the water vapor transport at levels below the surface pressure of the ice sheet p_*, the precipitation over the ice sheet can be computed from

$$P = E - \nabla \cdot \hat{f}(p_*) \vec{Q},$$

with Q calculated by using (11).

This parameterization of the vertical distribution of water vapor transport does not affect the total precipitation on the ice sheet. The poleward water vapor flux at the ice margin is not changed by the surface elevation. All of the water vapor transported across the ice margin must fall on the ice sheet as precipitation, though not necessarily as snow. The correction for elevation simply concentrates the snowfall along the equatorward margin of the ice sheet.

This simple parameterization has major limitations, especially when used in an energy balance model instead of with the observed heat flux. Energy balance models can produce realistic zonal-mean temperatures, but the diffusive heat transport must in some way include both the meridional transport of sensible and latent heat by the atmosphere and the oceanic heat transport. The water vapor flux parameterization requires the sensible heat flux alone. In middle latitudes the sensible heat flux is roughly half the total energy flux. Therefore, one can expect that the model will overestimate the water vapor transport by about a factor of two in middle latitudes.

2.3. *Coupling the energy balance model to an ice sheet model*

The ice sheet affects the energy balance model by reducing the surface air temperature over land and changing the surface energy fluxes. The surface air temperature is calculated by extrapolating from the atmospheric temperatures in the two layers to the surface pressure p_*, which is assumed to decrease exponentially with altitude with a scale height of 8 km. Except for its elevation, the ice sheet is treated as snow cover. In particular, all meltwater on the ice sheet is assumed to run off immediately.

The presence of the ice sheet would also affect the longwave radiation fluxes, which could possibly change the sensitivity of the model. This has not been accounted for in this model, but the magnitude of the effect can be estimated. The decrease in upward longwave is well accounted for by the present parameterization. Changes of the downward IR flux have been calculated by using a radiative transfer model. The annual-mean zonal-mean temperature profile from 75° N was used as input. If the clouds remain at constant σ levels ($\sigma = p/p_*$), the decrease is ~16 W m^{-2} km^{-1}, averaged over the lower 5 km. If clouds are fixed at constant pressure levels, and removed as the surface rises through them, the decrease is 22 W m^{-2} km^{-1}. This decrease is larger because the downward IR emitters (the cloud layers) are successively removed.

The sensitivity of the surface temperature to these changes in the downward IR can be estimated by assuming the insolation, surface air temperature, and latent heat flux are fixed. (The latent heat flux is small on the ice sheet.) The change in the downward IR must be compensated by changes in the upward blackbody radiation and the sensible heat fluxes from the surface. By linearizing the Stefan-Boltzmann equation the change in the surface temperature resulting from a change in the downward IR of 1 W m^{-2} can be estimated from (5) to be ~0.1 °C. Therefore, the surface temperature should respond to the decreased IR by cooling ~1.5 to 2 °C km^{-1}.

In the model the lapse rate in high latitudes lies in the range of 3 to 5 °C km^{-1}. The decrease of the *surface* temperature with elevation ranges from 2 to 4 °C km^{-1}. If the effect of surface elevation on the downward IR were included, the decrease of surface temperature would be nearer the atmospheric lapse rate. In sum, the model overpredicts the surface temperature of the ice sheet by ~1.5 to 2 °C km^{-1}, and consequently overpredicts the outgoing longwave radiation to space. This error could be important in simulating an Antarctica-like polar ice sheet with a high zonal-mean elevation. In this model the land fraction of 30% limits the elevation-radiation effect. In this case the error in the sensitivity caused by leaving the downward IR uncorrected is probably not major.

An ice sheet will undoubtedly have an effect on the meridional transport of heat as well. The Antarctic ice sheet certainly blocks the zonal-mean transport of heat at lower levels in the atmosphere. The Laurentide and Scandanavian ice sheets may have actually increased the meridional heat transport, at least in certain latitudes, by inducing large amplitude stationary waves or by enhancing cyclogenesis and transport by transient waves. Because it is not clear how to parameterize the effects of either a zonally symmetric ice sheet (similar to Antarctica) or zonally asymmetric ice sheets (such as existed in the northern hemisphere during the last ice age), the ice sheets are assumed to have no direct effects on the meridonal heat transport.

An ice sheet is assumed to be centered on each pole, maintaining the model's symmetry. Assuming that ice is a perfectly plastic material, the latitudinal profile of the ice sheets is given by

$$h(\theta,\theta_0) = \lambda\,(|\theta - \theta_0|)^{\frac{1}{2}}, \tag{13}$$

where θ_0 is the latitude of the ice sheet margin (Weertman, 1976). A value of $\lambda = 1000$ m (degree latitude)$^{-1/2}$ gives a central elevation of ~4500 m for an ice sheet extending to 70° latitude. The elevation of the entire land fraction at each latitude is equal to the ice sheet elevation.

The latitudes of the ice sheet margins are specified, then the energy balance model is integrated to equilibrium from an initially isothermal state. The annual net snow budget $B(\theta)$ is then calculated from the total annual snowfall $P(\theta)$ and ablation $A(\theta)$. The mass budgets of the ice sheets are then calculated by integrating B over the ice sheets. For the ice sheets to be in equilibrium, B must satisfy

$$M = \int_{\theta_0}^{\pi/2} B(\theta)\cos\theta\,\mathrm{d}\theta = 0. \tag{14}$$

If the mass budget M is positive, the ice sheet must be smaller than its equilibrium size for this solar constant; if M is negative, the ice sheet must be too large. The equilibrium climate is found by iterating on θ_0. The resulting mass budget information also indicates the rate of growth or shrinkage of the ice sheet near the equilibrium points and provides information on the stability of the equilibria.

3. Sensitivity of the model with snow cover

3.1 *Prescribed precipitation rates*

A simple precipitation parameterization, useful for understanding the effects of the snowfall rate on the sensitivity of the model, is to assume that the precipitation rate is independent of latitude and time. When the surface temperature falls below freezing, snow accumulates at the prescribed precipitation rate. If the annual accumulation (snowfall + frost accumulation) is greater than the ablation (snowmelt + sublimation), snow accumulates from year to year producing a permanent snow cover. Otherwise, snow disappears during the melt season.

The model generates a seasonally varying snow line in response to the seasonal cycle of temperature. The minimum extent of snow cover, which occurs in late summer, determines the equilibrium or permanent snow line. At this latitude the annual accumulation is equal to the annual ablation. The winter snow line is the latitude of the maximum equatorward extent of snow cover.

If the snowfall rate is low, the wintertime snow accumulation is shallow and melts rapidly when the temperature rises to freezing. In this case the albedo is essentially temperature dependent. A higher snowfall rate, however, produces a deeper snow cover, which requires longer to melt. This persistence of the snowcover introduces an albedo feedback that is lacking in the simple temperature-dependent case.

The seasonal range of snow cover in the model is plotted as a function of solar constant in Fig. 3 for two different values of the precipitation rate, a low value of 100 mm yr^{-1} and a high value of 500 mm yr^{-1}. The solar constant is expressed as a multiple of the present solar constant, 1376 W m^{-2}. The seasonal range of sea ice, which is the same in both cases, is much less than that of snow cover because the large heat capacity of the ocean mixed layer reduces the amplitude of the seasonal cycle of temperature.

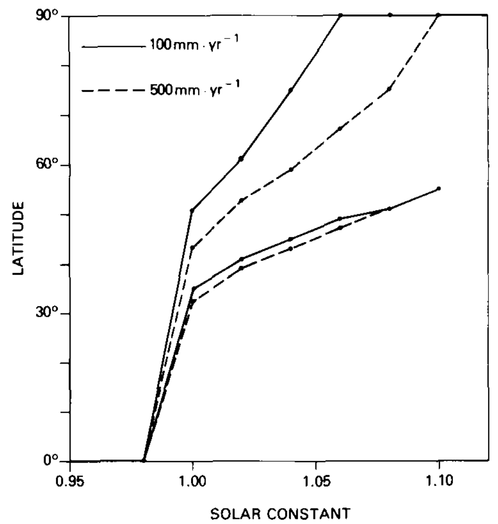

Fig. 3. Latitude of winter and summer (equilibrium) snow line as a function of solar constant for two values of the precipitation rate.

Changing the snowfall rate displaces the winter snow line only slightly, because the ablation rate at lower latitudes (reaching 10 m yr^{-1}) is much larger than the accumulation rate. As a result, temperatures in the tropics and subtropics are similar in the two cases. The permanent snow cover, however, is more extensive in the high precipitation case. At higher latitudes, the greater snow accumulation requires longer to melt, lowering temperatures.

Fig. 3 shows that the snowfall rate affects the sensitivity of the model (the slope of the equilibrium curves) as well as the equilibrium climate itself. The difference in sensitivity is due to the latitudinal gradient of the ablation rate, which is determined primarily by the air temperature and insolation. In polar latitudes the gradients of temperature and insolation are small. Therefore, the equilibrium snowline must move poleward or equatorward a large distance to re-establish equilibrium if the snowfall rate is changed. In middle latitudes the gradients of the air temperature and insolation, and therefore the ablation rate, are larger. Therefore, only a small change in the latitude of the equilibrium snowline is needed to balance a change of the accumulation rate, and the slope of the equilibrium curves must depend on the precipitation rate.

A latitudinal gradient of the precipitation rate could also affect the model sensitivity. This can be inferred from Fig. 3 by considering the results of gradually changing the precipitation rate from a high to a low value or vice versa as the solar constant is varied. If the precipitation rate increases as the solar constant decreases (equivalent to the precipitation rate increasing toward the equator), the equilibrium snow line will move from the higher equilibrium curve to the lower one and the sensitivity will be increased. If the precipitation rate at the snow line decreases, the reverse will be true.

The accumulation rate is therefore important in determining the equilibrium snow line latitude when the permanent snow cover is small, but less important when the permanent snow cover is extensive. A somewhat counter-intuitive corollary is that climates with high snowfall rates are less sensitive to changes in the solar constant than climates with lower snowfall rates. This is true only because the high precipitation rate allows a small permanent snow cover to exist for high solar constants.

3.2. *Predicted precipitation rates*

The ability of the model to simulate the observed zonal-mean hydrologic cycle is shown in Fig. 4 and 5. The annual-mean water vapor flux predicted by the model is shown in Fig. 4a along with the observed flux. The permanent snowline lies at 63° latitude. As expected, the model overpredicts the water vapor transport in middle latitudes by approximately a factor of two. The model also completely fails to represent the ITCZ.

The predicted and observed evaporation are shown in Fig. 4b. Model values include sublimation. Sellers (1965) does not state whether his estimates of evaporation include sublimation. Because the model overpredicts the permanent snow cover in high latitudes it underpredicts the evaporation rate. The observed evaporation rate falls from ~400 mm yr^{-1} at 60° N to ~0 at the pole. The model predicts essentially zero evaporation throughout this latitude zone. The annual-mean global-mean evaporation rate is 861 mm yr^{-1} in the model, compared to the observed global mean precipitation of ~1000 mm yr^{-1}.

When precipitation is computed from (10), the

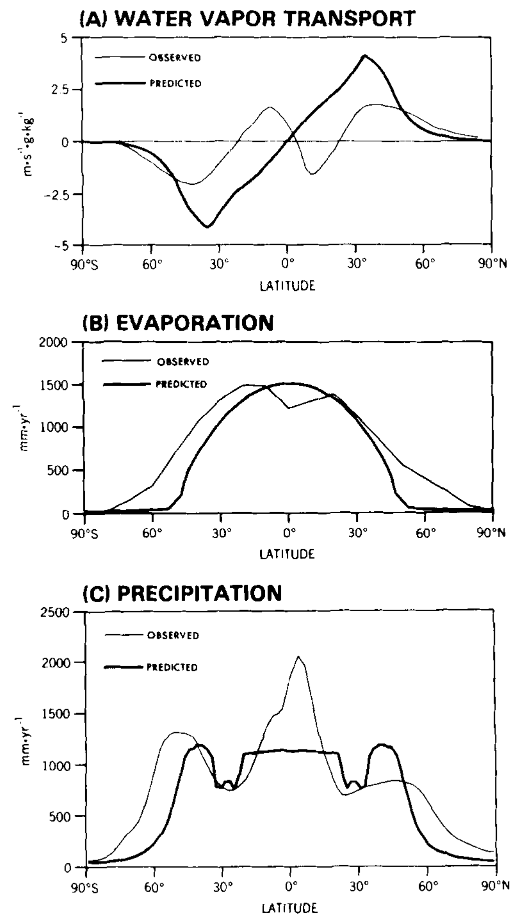

Fig. 4. Observed and predicted annual-mean meridional water vapor transport (A), evaporation (B), and precipitation (C). The observed water vapor transport is from Oort (1983), the evaporation from Sellers (1965, p. 84), and the precipitation from Jaeger (1976).

overestimate of the water vapor transport and the underestimate of the evaporation cancel to some extent in high latitudes. The precipitation rate predicted by the model can be compared to the observed rate in Fig. 4c. The agreement at high latitudes between the observed and predicted precipitation is better for a solar constant of 1.08 (see Fig. 6) because the hydrologic cycle becomes more intense and the precipitation increases. However, when the solar constant is raised the permanent snow cover disappears.

The predicted snowfall rate as a function of time and latitude is shown in Fig. 5. The maximum

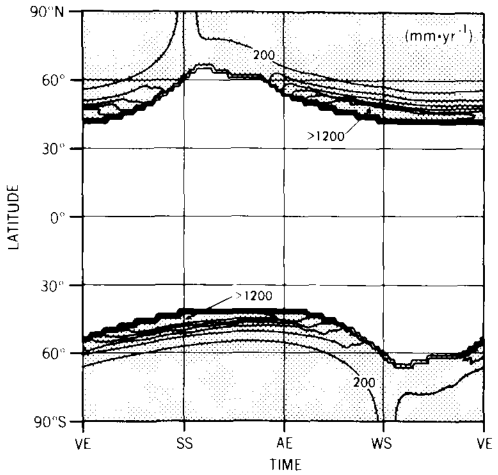

Fig. 5. Snowfall rate predicted by the model as a function of latitude and time. The abbreviations are vernal equinox (VE), summer solstice (SS), autumnal equinox (AE), and winter solstice (WS). The snowfall rate is largest near the snow margin and decreases toward the poles. In the unshaded region temperatures are never cold enough for snow to fall.

snowfall rate near the equatorward edge of the snowfall area is ~1200 mm yr^{-1}. The snowfall rate at the pole is less than 200 mm yr^{-1} during the winter. In the tropics the divergence of the water vapor flux is small, and the precipitation is roughly equal to the evaporation.

The broad minimum in the precipitation centered around 30° latitude is not a physically realistic feature. This minimum is an artifact produced by a discontinuity in the meridional temperature gradient. The convective adjustment in the tropics and summertime subtropics moves heat locally from the lower to the upper layer. This changes the meridional temperature gradient in both layers from the smooth diffusive value. The result is a discontinuity in the temperature gradient at the boundary between the convectively stable and unstable regions. The result is a large divergence in the heat transport, and therefore in the water vapor transport, at the boundary between the stable and unstable regions. This boundary shifts back and forth during the seasons, producing the broad minima seen in the annual-mean precipitation. This feature of the predicted precipitation is not important to the sensitivity of the model because the atmosphere is not convectively unstable in regions cold enough for snow to fall. The snowfall rate is therefore unaffected by the discontinuity in the temperature gradient.

The source of precipitation in polar latitudes is considerably different from that in the tropics. If the surface is snow or ice covered, the evaporation rate is low. Precipitation is therefore supplied almost exclusively by water vapor transported poleward in the atmosphere. The result is a rapid decrease in the precipitation poleward from the edge of the seasonal snow or ice cover. This is caused by both the dependence of the saturation vapor pressure on temperature and by the convergence of the water vapor flux associated with the convergence of the heat flux. In this region the latitudinal gradient of the predicted precipitation rate is very similar to that of the observed precipitation.

With this precipitation parameterization, changing the solar constant will change not only the fraction of the annual precipitation falling as snow (by changing the temperature), but the precipitation rate itself. Fig. 6 shows the annual-mean precipitation rate for two different values of the solar constant and the snowfall rate in each case. There is no permanent snow cover for the higher solar constant (1.08). The winter snow cover extends to 51° latitude. With a 4% decrease in the solar constant to 1.04 the equilibrium snowline jumps to 67°, and the winter snowline advances to 43°. The maxima in precipitation and snowfall are of comparable magnitude in both cases, but are shifted equatorward in the colder case. Precipitation decreases more than snowfall because the larger, summertime precipitation is eliminated by the cold atmosphere temperatures above the permanent snow cover. In the colder case all precipitation

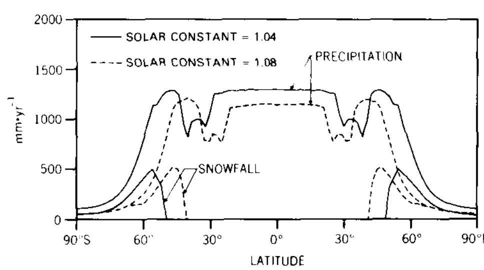

Fig. 6. Predicted annual-mean precipitation and snowfall for two values of the solar constant.

poleward of the equilibrium snowline falls in the form of snow.

Wetherald and Manabe (1975) have discussed the changes in the hydrologic cycle of a general circulation model resulting from a change in the solar constant. In the GCM a 6% reduction of the solar constant causes a significant decrease in the precipitation and evaporation rates. The intensity of the hydrologic cycle decreases because less energy is available at the surface for evaporation and because the dependence of the saturation mixing ratio on the temperature is weaker at lower temperatures. Conversely, when the solar constant is raised, there is a noticeable decrease in the snowfall rate in high latitudes despite an increase in the precipitation rate. In both the EBM and the GCM, the snowfall fraction in high latitudes changes abruptly when the solar constant is changed. Snow comprises about half of the annual precipitation at the higher solar constant. At the lower solar constant, essentially all of the annual precipitation poleward of 60° latitude falls in the form of snow in both models. The snowfall fraction decreases rapidly equatorward from the permanent snowline.

The change of the evaporation rate in both models is a smoother function of latitude than the precipitation rate. The evaporation rate changes abruptly only where the permanent snow cover advances or retreats.

Raising the solar constant does increase the precipitation rate, which could lead to more snowfall in high latitudes, as originally proposed by Simpson (1938). However, warmer temperatures mean that snow falls for a shorter period during the year and melts faster during the ablation season. The net result is a decrease in the snow cover.

The overall sensitivity of the snow cover in the model with the water vapor transport parameterization is plotted in Fig. 7. The snowfall rate at the equilibrium snow line for each solar constant is listed in Table 3. Snowfall rates are large near the seasonally varying snow margin (> 1000 mm yr^{-1}, see Fig. 7), but much lower at the *equilibrium* snow line (~150 to 325 mm yr^{-1}).

The snowfall rates at the equilibrium snow line lie between the two fixed values used in the previous section. As a result the equilibrium snow line resulting from the predicted snowfall lies within the range of the two cases with uniform precipitation (100 and 500 mm yr^{-1}).

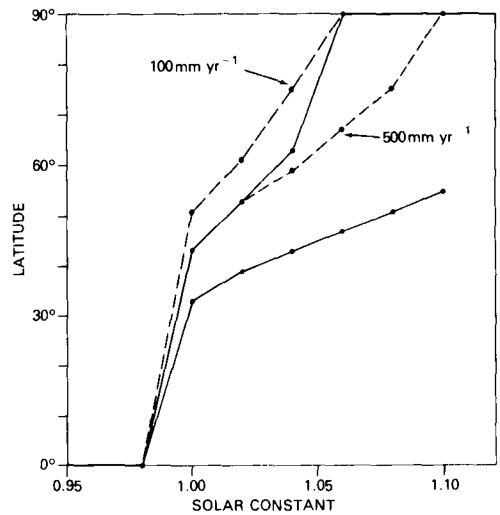

Fig. 7. Latitudes of winter and summer (equilibrium) snow lines as a function of solar constant for the model with predicted precipitation (solid lines) and for constant precipitation.

Table 3. *Annual snowfall rate at the equilibrium snow line*

Solar constant	θ_e (degrees latitude)	Snowfall rate (mm yr^{-1})
1.06	90	40
1.04	62	147
1.02	52	240
1.00	42	328

The snowfall parameterization produces snowfall rates at the equilibrium snow line with only mild dependence on solar constant. Therefore, the parameterization does not introduce strong feedback into the albedo-temperature feedback loop, but does make the model somewhat more sensitive than the uniform precipitation rate.

4. Sensitivity of the model with ice sheets

4.1. *Prescribed precipitation rates*

The latitude of the equilibrium ice margin was calculated as a function of solar constant for the same precipitation rates used with snow cover, 100 and 500 mm yr^{-1}. Fig. 8a and b show the

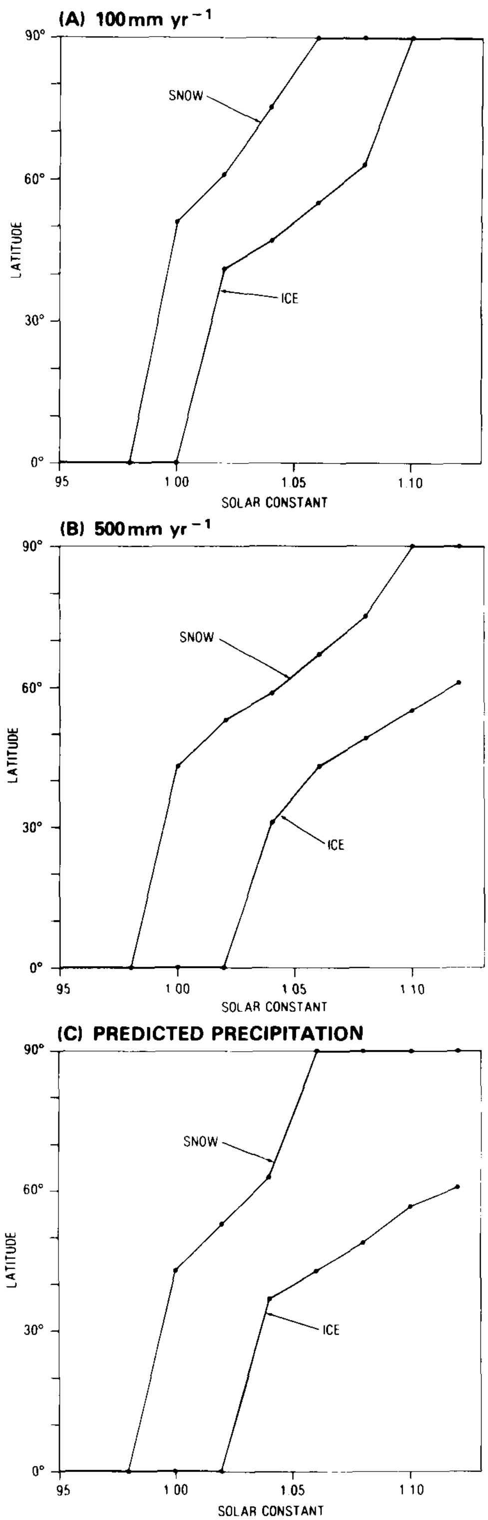

equilibrium curves for the two constant precipitation values. The curve labeled SNOW is for snow cover only, shown earlier in Fig. 3. The differences between the model with snow cover and with the ice sheet can be clearly seen in the figures. In both cases the ice sheet is significantly larger than the snow cover for all values of the solar constant. The explanation for the difference is straightforward. Because the ice sheet surface elevation is high, the surface temperature is colder than at sea level. The cold temperatures prevent the ice from melting, so the interior of the ice sheet lies entirely in the accumulation zone. The ice sheet must extend into lower latitudes than snow cover to be ablated and balance the mass budget. This effect can be duplicated in annual-mean models by using a higher value for the annual-mean temperature at the ice margin.

In the first case with precipitation at 100 mm yr^{-1} (Fig. 10), the ice sheet is slightly less sensitive than snow cover in middle latitudes. However, the ice sheet seems to have little net effect on the sensitivity of the model. The ice sheet introduces two factors into the seasonal model that could possibly change the model sensitivity: the elevation-radiation effect and the mass budget of the ice sheet. For reasons discussed below these effects do not manifest themselves in the model sensitivity.

The elevation-radiation effect discussed in Bowman (1982) should reduce the sensitivity when the ice sheet is included. Two factors prevent the elevation-radiation effect from having the magnitude seen in the annual-mean model. First, the land fraction is set to 0.3 everywhere. Therefore, the elevation-radiation effect is reduced to 30% magnitude if the ice sheet were to occupy 100% of a latitude circle. For this reason alone the importance of the elevation-radiation effect is much reduced in the seasonal model. Secondly, the smaller effective lapse rate in this model (3 to 5 °C km^{-1} as compared to 6.5 °C km^{-1} in the annual-mean model), as well as by the neglect of the

Fig. 8. Sensitivity of the energy balance model with constant precipitation rates of 100 mm yr^{-1} (A) and 500 mm yr^{-1} (B), and with predicted precipitation rates (C). The curves labeled SNOW indicate the equilibrium snow line for each case as shown earlier in Figs. 3 and 7. The curves labeled ICE are the latitude of the margin of the ice sheet as a function of solar constant.

change in the downward IR caused by the surface elevation, both reduce the elevation-radiation effect. The elevation-radiation effect is proportional to $b\Gamma z_*$, where b is the coefficient of the temperature dependent part of the IR cooling parameterization, Γ is the lapse rate, and z_* is the surface elevation. The combined effects of the small land-area fraction and the comparatively warm ice sheet surface temperatures together should reduce the strength of the elevation-radiation effect by approximately a factor of six, almost eliminating the elevation-radiation effect as a part of the feedback processes of the model.

Whether the mass budget acts as a model feedback depends on the ratio of the mean accumulation rate in the accumulation zone to the mean ablation rate in the ablation zone. A low ratio of accumulation to ablation implies a large accumulation zone and a small ablation zone for an equilibrium ice sheet. The ice margin is closely tied to the equilibrium snowline and the ice sheet does not affect the model sensitivity. This relationship is discussed in the Appendix and illustrated with a simple annual-mean energy balance model.

The actual annual-net mass budget as a function of latitude is shown in Fig. 9 for several values of the solar constant. These are taken from the model experiments with a precipitation rate of 500 mm yr^{-1}. It can be seen that the ablation rate is much larger in magnitude than the accumulation rate. The steep latitudinal temperature gradient at the ice margin causes large amounts of sensible heat to be transported onto the ice sheet by the atmosphere from the ice free regions equatorward of the ice margin. The sensible heat transport and the high summer insolation produce the large ablation rates.

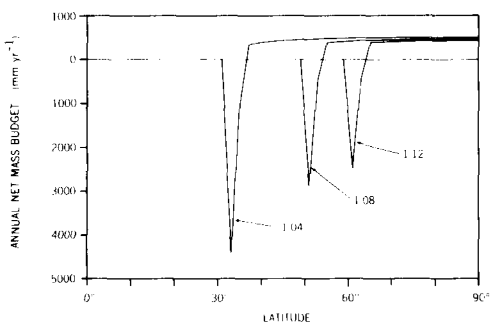

Fig. 9. Annual net mass budget of the ice sheet as a function of latitude as calculated by the energy balance model for three different values of the solar constant. The precipitation rate is 500 mm yr^{-1}.

In the model with the ice sheet and uniform precipitation rates the equilibrium curve is shifted toward higher values of the solar constant, but the sensitivity of the ice margin is only slightly less than that of snow cover.

4.2. *Predicted precipitation rates*

The sensitivity of the seasonal model with the ice sheet and the water vapor transport parameterization is plotted in Fig. 8c. In this case the sensitivity of the model with ice sheets is noticeably less than with snow cover alone. Because the elevation-radiation effect is comparatively weak, the differences must be caused by the adjustment of the hydrological cycle, and specifically by changes in the precipitation rate. Table 4 lists the mean snowfall rate over the ice sheet for each equilibrium value in the curve in Fig. 8c. With snow cover only the snowfall rate at the equilibrium snow line increases as the solar constant decreases (Table 3), acting as a positive feedback to the snow line. In the ice sheet case the snowfall rate over the ice sheet remains nearly constant despite changes in the solar constant. This results from the form of the mass budget and from concentrating the snowfall along the ice margin. Changing the ice sheet size has little effect on the snowfall rate. Maintaining a constant snowfall rate accounts for the slower decrease in ice sheet size as the solar constant is raised.

5. Discussion

These experiments with a simple numerical model indicate the possible importance of the latitudinal distribution of precipitation and the

Table 4. *Mean snowfall rate over the ice sheet*

Solar constant	θ_0 (degrees latitude)	Snowfall rate (mm yr^{-1})
1.12	61	380
1.10	57	353
1.08	49	374
1.06	43	364
1.04	37	348

seasonal cycle of snowfall and ablation in determining the sensitivity of climate. In high latitudes the equilibrium snow line can be sensitive to small changes in the snowfall rate or the solar constant. Through the albedo feedback a higher snowfall rate or lower solar constant causes a larger area of permanent snow cover. In middle latitudes the meridional gradients of temperature and ablation rate are larger. Only small adjustments of the equilibrium snow line are necessary to re-establish equilibrium. However, if the permanent snow cover becomes large enough, the model approaches the "large ice cap instability" (Held et al., 1981) and the snow line becomes more sensitive once again.

A latitudinal gradient of the precipitation rate can also affect the sensitivity of the equilibrium snowline. If the precipitation rate increases toward the equator, as is observed, the snow line is more sensitive than if the precipitation is constant with latitude. Reducing the solar constant advances the snow line into regions of greater snowfall, amplifying the albedo-temperature feedback.

The water vapor transport parameterization produces a substantial latitudinal gradient of the precipitation rate. The precipitation rate decreases when the solar constant is reduced. Nevertheless, the snow line moves equatorward into regions of higher precipitation. This latitudinal gradient of the precipitation rate makes the snow line somewhat more sensitive than when the precipitation rate is constant with latitude.

Adding the ice sheets to the model causes substantial changes in the extent of permanent snow and ice cover. The ice sheets are always much larger than permanent snow cover for equal values of the solar constant and precipitation rate. This is a consequence of the ice sheet's surface elevation, which lowers the surface temperature and prevents melting except near the ice margin. This result suggests that large ice sheets, especially polar ice sheets like that in Antarctica, are stable to changes in their mass budget because the ablation zone is confined to low elevation regions near the ice sheet margin.

If the precipitation rate is constant in time and latitude, the sensitivity of the ice sheet margin is similar to the sensitivity of the equilibrium snowline. Analysis of two major effects of ice sheets, the elevation-radiation effect and the mass budget of the ice sheet, suggest that they are weak feedback effects in this model and of opposite sign. The elevation-radiation effect is limited by the 30% land fraction. Mass budget effects are small because the ablation rate is large in comparison to the accumulation rate.

When the snowfall rate is calculated from the precipitation parameterization, however, the ice margin is less sensitive than the snow cover. This occurs because the snowfall rate adjusts differently in the two cases. The mean snowfall rate on the ice sheet remains nearly constant. Snow cover, on the other hand, experiences a positive feedback as the equilibrium snow line advances into latitudes where the snowfall rate is higher.

The changes in the hydrologic cycle predicted by the model generally agree with sensitivity experiments performed with general circulation models (e.g. Wetherald and Manabe, 1975). Raising the solar constant does increase the precipitation in high latitudes, as proposed by Simpson (1938), but the albedo-temperature feedback reduces the fraction that falls as snow and the total snow cover decreases. Therefore, raising the solar constant cannot lead to an ice age.

6. Acknowledgements

This work was performed while the author was a student in the Geophysical Fluid Dynamics Program, Princeton University. The assistance and advice of the students and faculty of the program, especially S. Manabe, I. Held, K. Moore, and J. Kinter, and the staff of the Geophysical Fluid Dynamics Laboratory, National Oceanic and Atmospheric Administration, is gratefully acknowleged. This paper benefited substantially from the reviewers' comments. Financial support was provided by the National Science Foundation under grant ATM 8106800. While preparing this paper the author was supported by a National Research Council Resident Research Associateship at NASA Goddard Space Flight Center.

7. Appendix

Including a snow budget in even a simple climate/ice sheet model can introduce additional feedbacks into the model. This is illustrated below with a simple annual-mean energy balance model and an equilibrium ice sheet. The model has one level, diffusive heat transport, a step-function albedo, and a linear radiation parameterization that includes corrections for the ice sheet surface elevation. The ice sheet is the same as that described in Section 2.3 (eq. 13). A complete description of the model can be found in Bowman (1982).

The snow budget B is assumed to be a function of the annual-mean temperature T

$$B(\theta) = \begin{cases} B_+ & T(\theta) < T_0 \\ B_- & T(\theta) > T_0 \end{cases} \tag{15}$$

The model must satisfy the constraint

$$T(\theta_e) = T_0, \tag{16}$$

where θ_e is the equilibrium snow line latitude, not the ice margin; and T is the surface temperature (not the sea level temperature). The equilibrium snow line lies in the interior of the ice sheet if the ice sheet is in equilibrium. The mass budget of the ice sheet M must satisfy (14). The step function form of the snow budget (15) allows (14) to be solved for θ_0 (the ice sheet margin) as a function of θ_e. The result is

$$\sin(\theta_0) = \delta + (1 - \delta)\sin(\theta_e), \tag{17}$$

where $\delta = B_+/B_-$ is the ratio of the average accumulation rate to the ablation rate ($\delta < 0$). The albedo is a step function at θ_0.

The model is solved by fixing θ_0 and calculating θ_e from (17). The solar constant is then adjusted iteratively to satisfy (16). The sensitivity of the ice margin depends in part on δ. In the limit in which the magnitude of B_+ is much less than B_-, $\delta \to 0$ and (17) reduces to $\theta_0 = \theta_e$. In this limit the equilibrium snow line lies at the ice margin, and the ice sheet behaves exactly like snow cover. As δ becomes increasingly negative, a small change in θ_e produces a progressively larger change in θ_0, because the ablation zone must increase in size. Because θ_e depends on the temperature and θ_0 determines the albedo, the mass budget amplifies the albedo-temperature feedback when $\delta < 0$. Fig. 10 shows the equilibrium ice sheet size as a function of solar constant for several values of δ. Increasingly negative values of δ make the ice margin more sensitive. The mass budget can counteract the stabilizing influence of the elevation-radiation effect if δ is of sufficient magnitude. It should be noted that with the assumed form of the snow budget, the mass budget of the ice sheet cannot act as a stabilizing influence because δ must be less than zero.

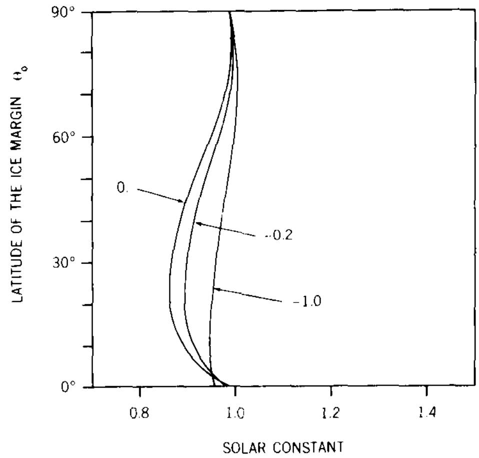

Fig. 10. Sensitivity of an annual-mean energy balance model with an ice sheet and the assumed form of the ice sheet mass budget (14). The latitude of the ice sheet margin as a function of solar constant is shown for three values of the mass budget parameter δ, which is defined as the ratio of accumulation to ablation.

REFERENCES

Birchfield, G. E., Weertman, J. and Lunde, A. T. 1982. A model study of the role of high-latitude topography in the climatic response to orbital insolation anomalies. *J. Atmos. Sci. 39*, 71–87.

Bowman, K. P. 1982. Sensitivity of an annual mean diffusive energy balance model with an ice sheet. *J. Geophys. Res. 87*, 9667–9674.

Budyko, M. I. 1969. The effect of solar radiation variations on the climate of the earth. *Tellus 21*, 611–619.

Gates, W. L. 1976. The numerical simulation of ice-age climate with a global general circulation model. *J. Atmos. Sci. 33*, 1844–1873.

Hays, J. D., Imbrie, J. and Shackleton, N. J. 1976.

Variations in the earth's orbit: pacemaker of the ice ages. *Science 194*, 1121–1132.

Held, I. M. and Suarez, M. J. 1974. Simple albedo feedback models of the icecaps. *Tellus 26*, 613–629.

Held, I. M. and Suarez, M. J. 1978. A two-level primitive equation atmospheric model designed for climatic sensitivity experiments. *J. Atmos. Sci. 35*, 206–229.

Held, I. M., Linder, D. I. and Suarez, M. J. 1981. Albedo feedback, the meridional structure of the effective heat diffusivity, and climatic sensitivity: results from dynamic and diffusive models. *J. Atmos. Sci. 38*, 1911–1927.

Jaeger, L. 1976. Monatskarten des niederschlags für die ganze erde. *Berichte des Deutsch Wetterdienstes*, Nr. 139, Offenbach a. M.

Kurihara, Y. 1973. Experiments on the seasonal variation of the general circulation in a statistical-dynamical model. *J. Atmos. Sci. 30*, 25–49.

Manabe, S. and Strickler, R. F. 1964. Thermal equilibrium of the atmosphere with a convective adjustment. *J. Atmos. Sci. 21*, 361–385.

Manabe, S. and Wetherald, R. 1967. Thermal equilibrium of the atmosphere with a given distribution of relative humidity. *J. Atmos. Sci. 24*, 241–259.

Milankovitch, M. 1941. *Canon of insolation and the ice age problem.* Royal Serbian Academy Publication 133, Belgrade, 633 pp., in Serbo-Croation (Translation, Israel Program for Scientific Translation, 1969, 482 pp.).

Mullen, A. B. 1979. *A mechanistic model for mid-latitude temperature structure.* Ph.D. thesis, Massachusetts Institute of Technology, Cambrdige, MA.

North, G. R. 1975. Analytical solution to a simple climate model with diffusive heat transport. *J. Atmos. Sci. 32*, 1301–1307.

North, G. R., Cahalan, R. F. and Coakley, J. A. 1981. Energy balance climate models. *Rev. Geophys. Space Phys. 19*, 91–121.

North, G. R., Mengel, J. G. and Short, D. A. 1983. Simple energy balance model resolving the seasons and the continents: application to the astronomical theory of the ice ages. *J. Geophys. Res. 88*, 6576–6586.

Oort, A. H. 1983. Global atmospheric circulation statistics, 1958–1973. *Professional Paper 14*, National Oceanic and Atmospheric Administration, Washington, DC, 180 pp.

Pollard, D., Ingersoll, A. P. and Lockwood, J. G. 1980. Response of a zonal climate-ice sheet model to the orbital perturbations during the quaternary Ice ages. *Tellus 32*, 301–319.

Sellers, W. D. 1965. *Physical Climatology*. University of Chicago Press, Chicago, IL, 242 pp.

Sellers, W. D. 1969. A global climatic model based on the energy balance of the earth-atmosphere system. *J. Appl. Meteorol. 8*, 392–400.

Simpson, G. 1938. Ice ages. *Nature 141*, 591–598.

Stone, H. M. and Manabe, S. 1968. Comparison among various numerical models designed for computing infrared cooling. *Mon. Weather Rev. 96*, 735–741.

Suarez, M. J. 1976. *An evaluation of the astronomical theory of the ice ages.* Ph.D. thesis, Princeton University, Princeton, NJ, 108 pp.

Suarez, M. J. and Held, I. M. 1979. The sensitivity of an energy balance climate model to variations in the orbital parameters. *J. Geophys. Res. 84*, 4825–4836.

Weertman, J. 1976. Milankovitch solar radiation variations and Ice age ice sheet sizes. *Nature 261*, 17–20.

Wetherald, R. T. and Manabe, S. 1975. The effects of changing the solar constant on the climate of a general circulation model. *J. Atmos. Sci. 32*, 2044–2059.

Williams, J., Barry, R. G. and Washington, W. M. 1974. Simulation of the atmospheric circulation using the NCAR global circulation model with ice age boundary conditions. *J. Appl. Meteorol. 13*, 305–317.